Supplementary Information

Gold nanoclusters adjuvant enables the eradication of persister cells by antibiotics and abolishes the emergence of resistance

Zhixin Cao[1, 2] Xiaohua Chen[1, 3], Jing Chen[1], Anping Xia[1], Brian Bacacao[1], Jessica Tran[1], Devesh Sharma[1], Laurent A. Bekale[1*], and Peter L. Santa Maria[1*]

[1]Department of Otolaryngology, Head and Neck Surgery, Stanford University, 801 Welch Road Stanford, CA 94305-5739, USA

[2]Department of Pathology, Shandong Provincial Hospital Affiliated to Shandong First Medical University, China

[3]Department of Otolaryngology-Head and Neck Surgery, the First Affiliated Hospital, Zhengzhou University, Zhengzhou 450000, China

[1] The Protein and Nucleic Acid Biotechnology Facility, Beckman Center Stanford University, 279 Campus Drive West Stanford, CA 94305

*Corresponding author. E-mail: bekale20@stanford.edu, petersantamaria@stanford.edu.

Materials and methods

Synthesis of cell-penetrating peptide (CPP)

Ac-YGRKKRRQRRR-(β-Ala)-(β-Ala)-(β-Ala)-Cys-CONH2 (CPP) was synthesized using an ABI 433A automatic peptide synthesizer on a 0.25 mmol scale by standard fluorenylmethyloxycarbonyl (Fmoc) solid-phase peptide synthesis (SPPS) on a Novabiochem NovaPEG Rink Amide resin. Post peptide synthesis, an acetyl group was coupled manually onto the N-terminus by adding Oxyma Pure and acetic anhydride in N, N-dimethylformamide (DMF). The Peptidyl resin was washed with N, N-dimethylformamide (DMF) and dichloromethane (DCM) and then dried. The modified peptide was cleaved from the resin with a trifluoroacetic acid (TFA)/Phenol/triisopropylsilane (TIS)/water cleavage cocktail. The peptide was purified using the Waters system by reverse-phase high-performance liquid chromatography (RP-HPLC). The molecular masses were determined by MALDI-TOF using the Voyager-DE RP Biospectrometry Workstation instrument.

Cell culture and in vitro cytotoxicity assay

The human lung adenocarcinoma cell line (A549) was maintained in DMEM (Dulbecco's modified Eagle's medium) supplemented with 10% fetal bovine serum (FBS) and 1% penicillin. The cells were incubated in 5% CO_2 humidified at 37 °C for growth. The cytotoxicity induced by AuNC@CPP was investigated by 3-(4,5-dimethylthiazol-2-yl)-2,5-diphenyltetrazolium bromide (MTT) assay. A549 cells (2×10^4/mL, 100 μL/well) were seeded in 96-well plates. After 24 h, the cell culture was exposed to concentrations of AuNC@CPP ranging from 0 μg/mL to 3200 μg/mL (AuNC@CPP were dispersed in DMEM). After 24 h of incubation, the medium containing AuNC@CPP was removed, cells were washed with PBS and incubated with fresh cell culture medium for another 24 h. Then, 20 μL of the MTT (5 mg/mL) was added to each well and incubated for 4 h in 5% CO_2 humidified at 37 °C. The medium was removed carefully, and 200

μL of dimethyl sulfoxide (DMSO) was added to each well to dissolve formazan crystals. The absorbance of formazan was read at 595 nm using the microplate reader. A blank solution (0 μg/mL of AuNC@CPP) was tested, and no cytotoxicity could be observed. Three independent experiments and 4 replicates were performed. Results were analyzed as the average viability (% of the untreated control) ± Standard deviation (SD).

Measurement of total thiol pool

Stationary overnight phase cultures of PA01 and SA 25923 were treated with and without AuNC@CPP (800 μg/mL) treatment for 2 h. According to the manufacturer's instructions, the thiol level was measured using a fluorometric free thiol assay kit (Abcam).

Step-wise treatment

CCCP-induced persister cells were challenged with OFL (10 μg/mL) or TOB (40 μg/mL) OFL (10 μg/mL) plus AuNC@CPP (800 μg/mL) for 24 h. After the survival bacteria were washed 3x with PBS, the pellet was resuspended in 100 μL of PBS and then spread on an LB plate. The plate was incubated for 72 h at 37 °C before assessing growth.

Disc diffusion assay

Strains of PA01 and SA 25923 were tested for susceptibility against ofloxacin using the disc diffusion method according to the Clinical Laboratory Standard Institute (CLSI) guidelines. In brief, glycerol stocks of each bacteria were streaked on LB plates and grown overnight at 37 °C. An inoculum was then prepared by taking several individual colonies and diluting in PBS with a 0.5 McFarland Standard turbidity. The inoculum was then spread with sterile cotton swabs on Mueller Hinton agar plates supplemented with 5% sheep blood. Discs containing 5 μg of ofloxacin

(Oxoid) were dispensed on the surface of the plate. For gold nanoclusters, 20 µL from an 800 µg/mL solution was dispensed drop-wise on a blank sterile 6 mm disc. After 24 h incubation at 37 °C, the inhibition zone was measured using a digital calliper.

Formation of AuNC@CPP protein coronas and assessment of antipersister activity

AuNC@CPP was incubated in 10% human plasma at 37 °C for 24 h to form the protein coronas (AuNC@CPP/coronas). CCCP-induced persisters cells of PA01 were then challenged with OFL (10 µg/mL) combined with either pristine AuNC@CPP (800 µg/mL) or AuNC@CPP/coronas (800 µg/mL). After 24 h, the survival bacteria were washed 3x with PBS. Then, the pellet was resuspended in 100 µL of PBS and spread on an LB plate. The plates were incubated for 72 h at 37 °C before assessing growth.

In vivo cytotoxicity

Animal Treatment and Sample Collection. All animal work was approved by Stanford University's Administrative Panel on Laboratory Animal Care. The 10−12 week-old C57BL/6J mice were purchased from Jackson Laboratories (Sacramento, CA) and housed in Stanford University's animal resource facility according to standard guidelines in which food and water were provided ad libitum in a room maintained at 12 h dark/light cycles. Male (n = 5 each group) C57BL/6J mice were divided into four groups, including control (PBS) and AuNC@CPP. The treatments were administrated by intraperitoneal (IP) injection at a single dose of 8 mg/kg (i.e., 0.8 mg/mL). At 24 h post-treatment, mice were sacrificed. Blood were collected for further investigation of the serum chemistry and hematology. Blood samples were subjected to toxicity analysis. An inferior vena cava blood collection was performed at the sacrifice. Blood (150 µL) was placed in a K2 EDTA tube for hematological analysis, and the left blood sample was placed in a 1.5 mL Eppendorf tube for serum extraction. The serum was separated by centrifuging the blood to remove the cellular fraction for liver and renal function testing.

Measurement of membrane potential using the fluorescent voltage reporters DiBAC4(3)

Bis-oxonol fluorophore, $DiBAC_3(4)$, is an anion whose fluorescent intensity depends on the membrane potential. After the depolarization, the dye enters the cell and exhibits an intense fluorescence. In contrast, as the membrane potential becomes more negative inside or hyperpolarized, cells become increasingly less permeable to $DiBAC_3(4)$, indicated by decreased fluorescence intensity. CCCP-induced persister cells (optical density 0.3) were treated with CCCP

(800 µg/mL), AuNC@CPP (800 µg/mL) and nigericin (8 µg/mL), respectively. Untreated and CCCP-induced persister cells treated with nigericin were used as a negative and positive control. After 3 h treatment at 37 ºC, the CCCP-induced persister cells were washed with PBS and incubated with 0.5 µM of $DiBAC_4(3)$ for 10 minutes at 25 °C. 100 µL of this solution was placed in 96-well black plates, and fluorescence intensity was measured using a plate reader at (Ex/Em: 490/516 nm).

Dissociation of mature biofilms

Overnight cultures of PA01 or SA 25923 were diluted 1:1,000 in fresh LB medium, and 150 µL was added to wells in an MBEC Assay®Biofilm Inoculator with 96 wells. Biofilms were allowed to develop onto peg lids for 48 h without shaking. The peg lids were gently rinsed to remove planktonic bacteria and incubated in a new MBEC Assay®Biofilm Inoculator with 96 wells containing AuNC@CPP (800 µg/mL) in PBS. PBS treated biofilm was used as the negative control. These MBEC Assay®Biofilm inoculators with 96 wells were incubated for 24 h. Then the peg lids were washed and stained with 0.1% Crystal Violet (CV) for 15 min. The remaining biofilm was quantified by CV absorbance intensity at 595 nm.

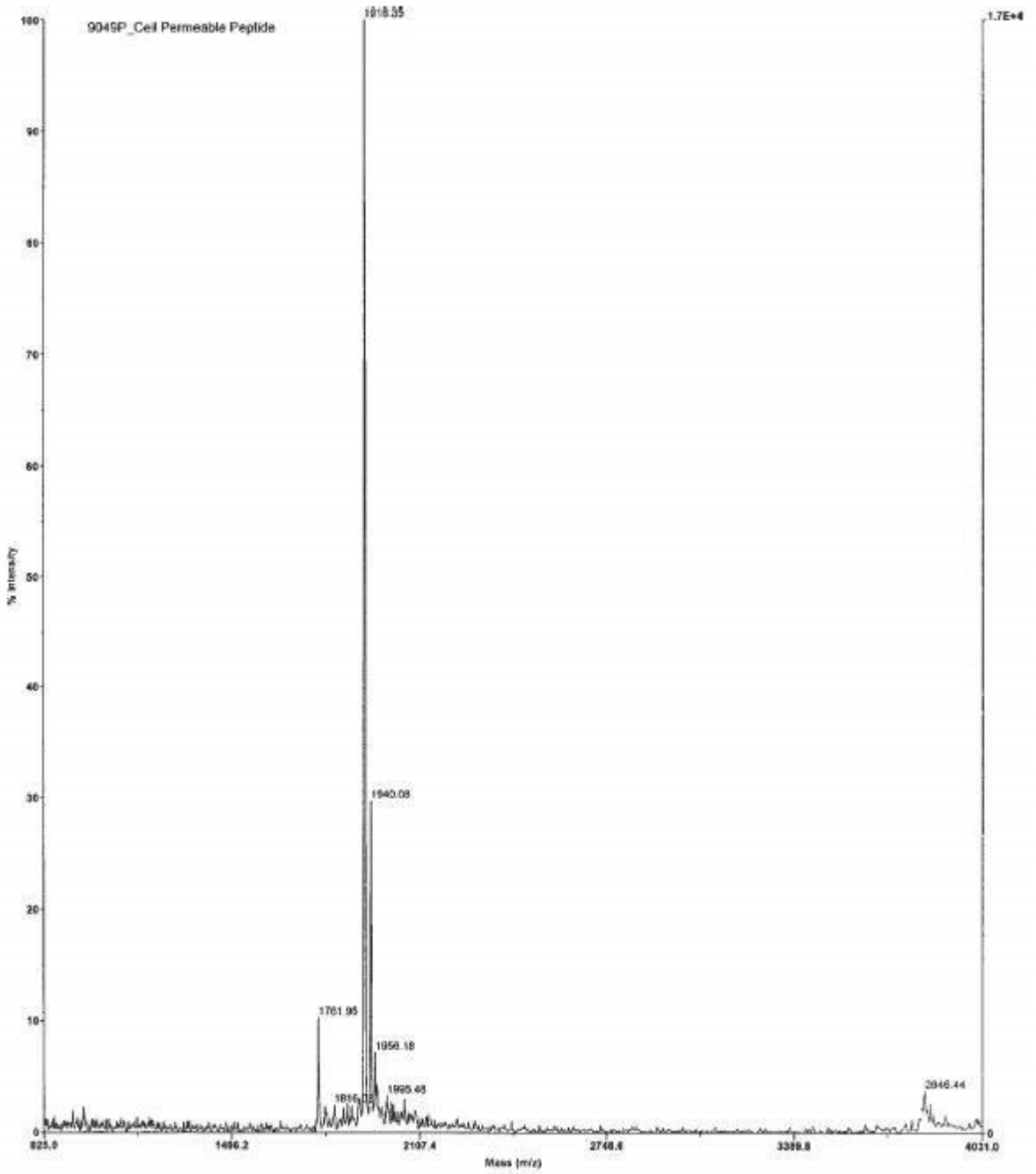

Fig. S1 High-resolution mass spectrum shows a peak at m/z 1918.13, which corresponds to the molecular weight of CPP

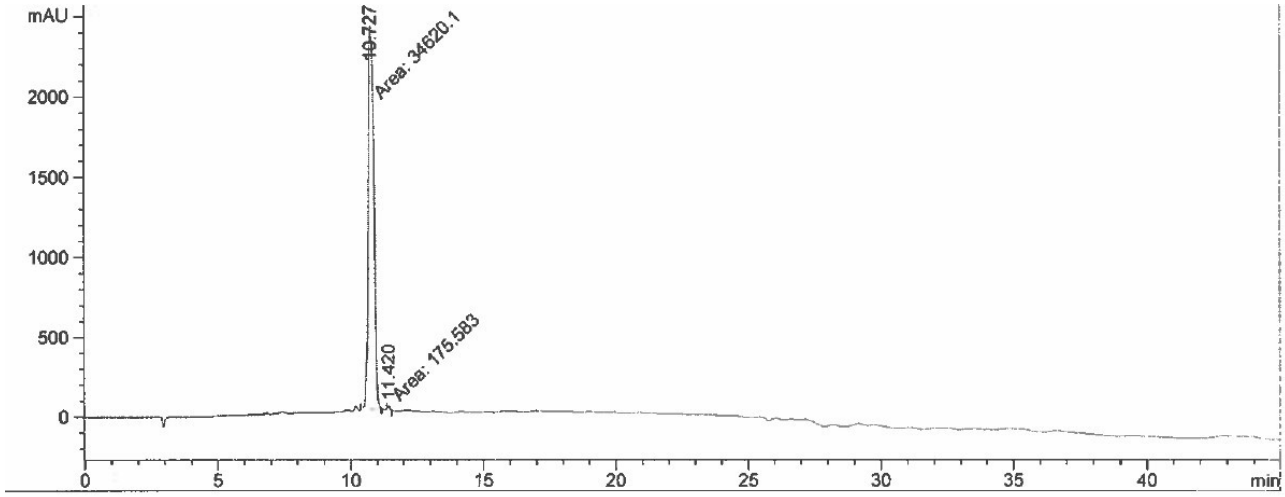

Fig. S2 CPP peak purity assessment in high-performance liquid chromatography (HPLC)

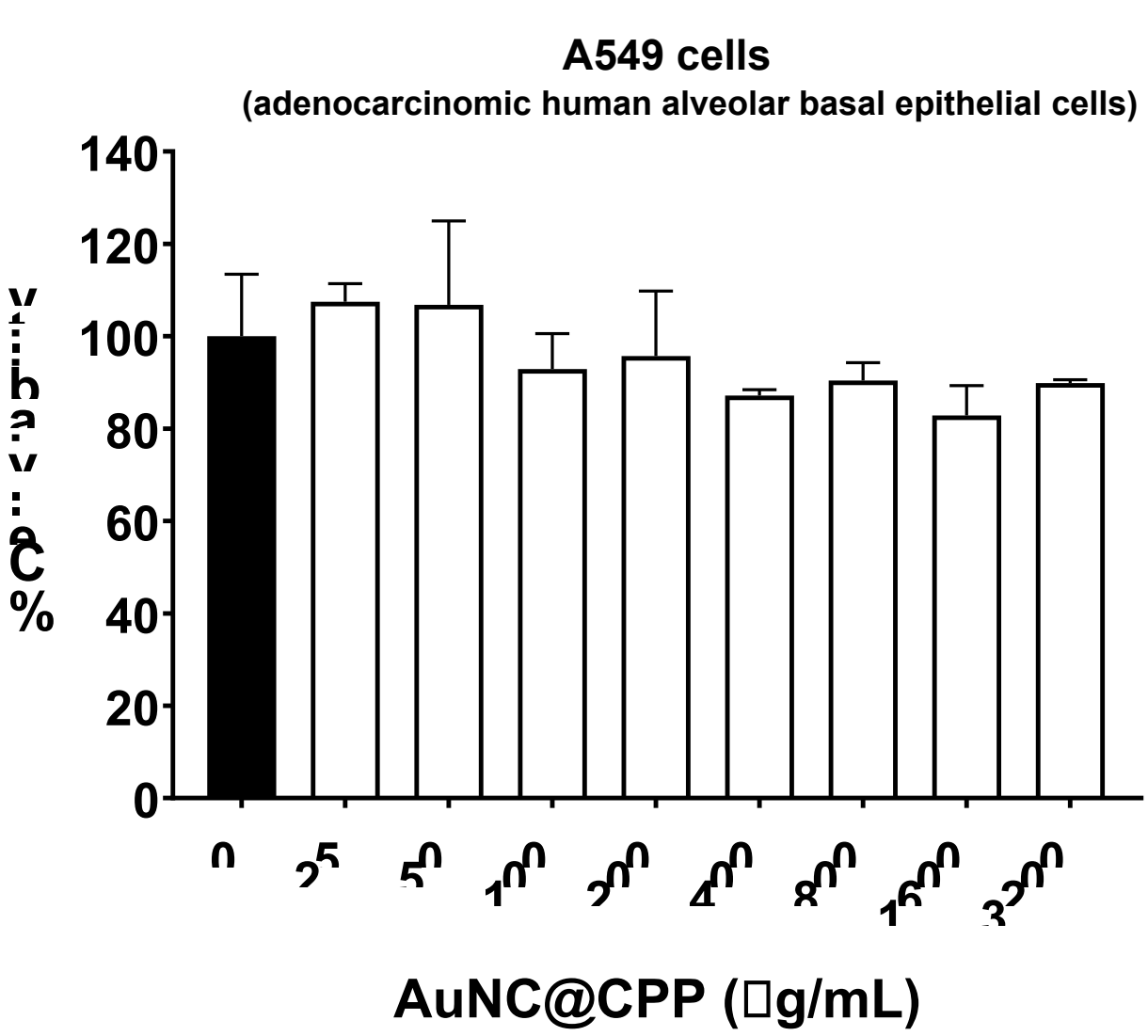

Fig. S3 Biocompatibility of AuNC@CPP. A549 cells were treated with AuNC@CPP for 24 h, and the cell viability was determined by MTT assay. Cells exposed with AuNC@CPP at 3200 μg/mL show more than 90% viable cells. Data are presented as mean ± s.d. (n= 4).

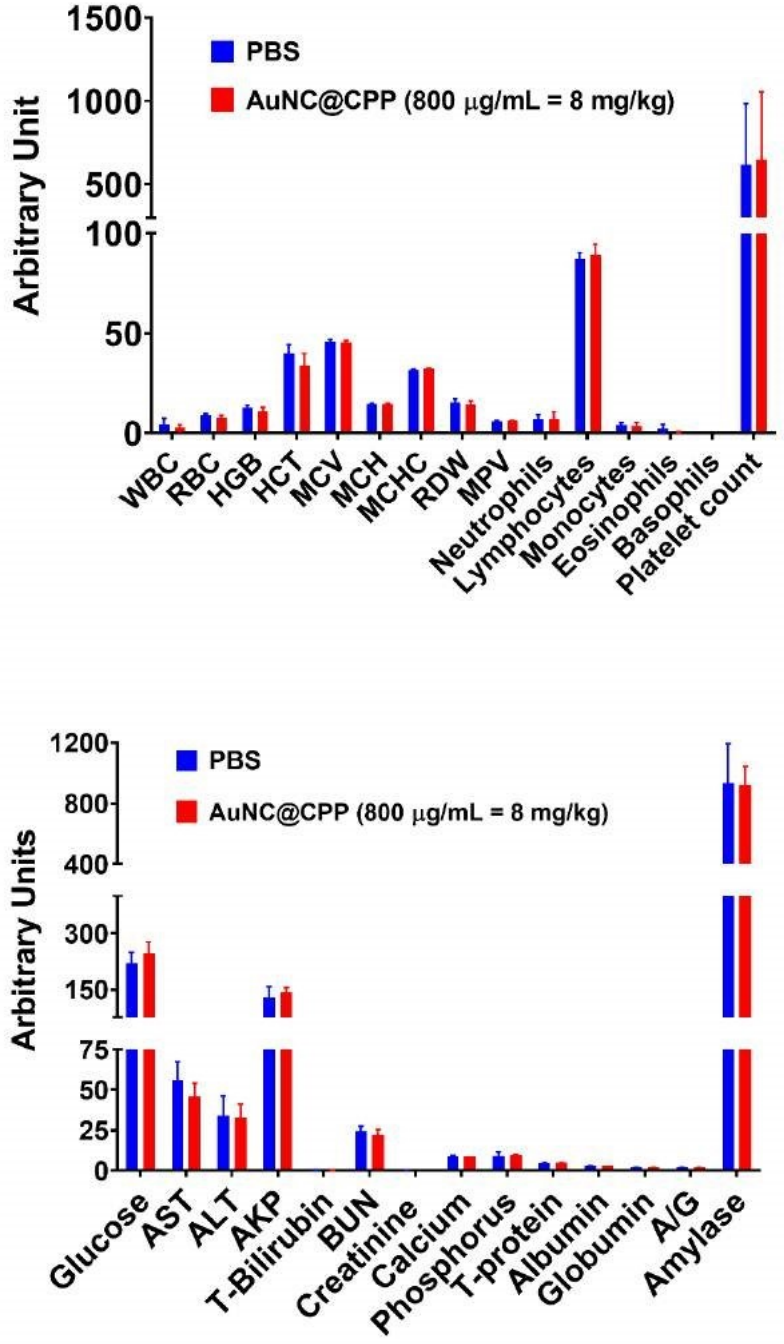

Fig. S4 In vivo biosafety of AuNC@CPP. Effect of AuNC@CPP on hematology and chemistry parameters at 24 h Post intraperitoneal at a Dose of 8 mg/kg. RBC: Red blood cell; HGB: Hemoglobin; MCV: Mean corpuscular volume; MCH: Mean cell haemoglobin; MCHC: Mean corpuscular hemoglobin concentration; WBC: White blood cells; MPV: Mean; RDW: Red cell distribution width; HCT: hematocrit; AST: Aspartate aminotransferase; ALT: Alanine aminotransferase; AKP: alkaline phosphatase; BUN: bood urea nitrogen; A/G: albumin/globulin ratio.

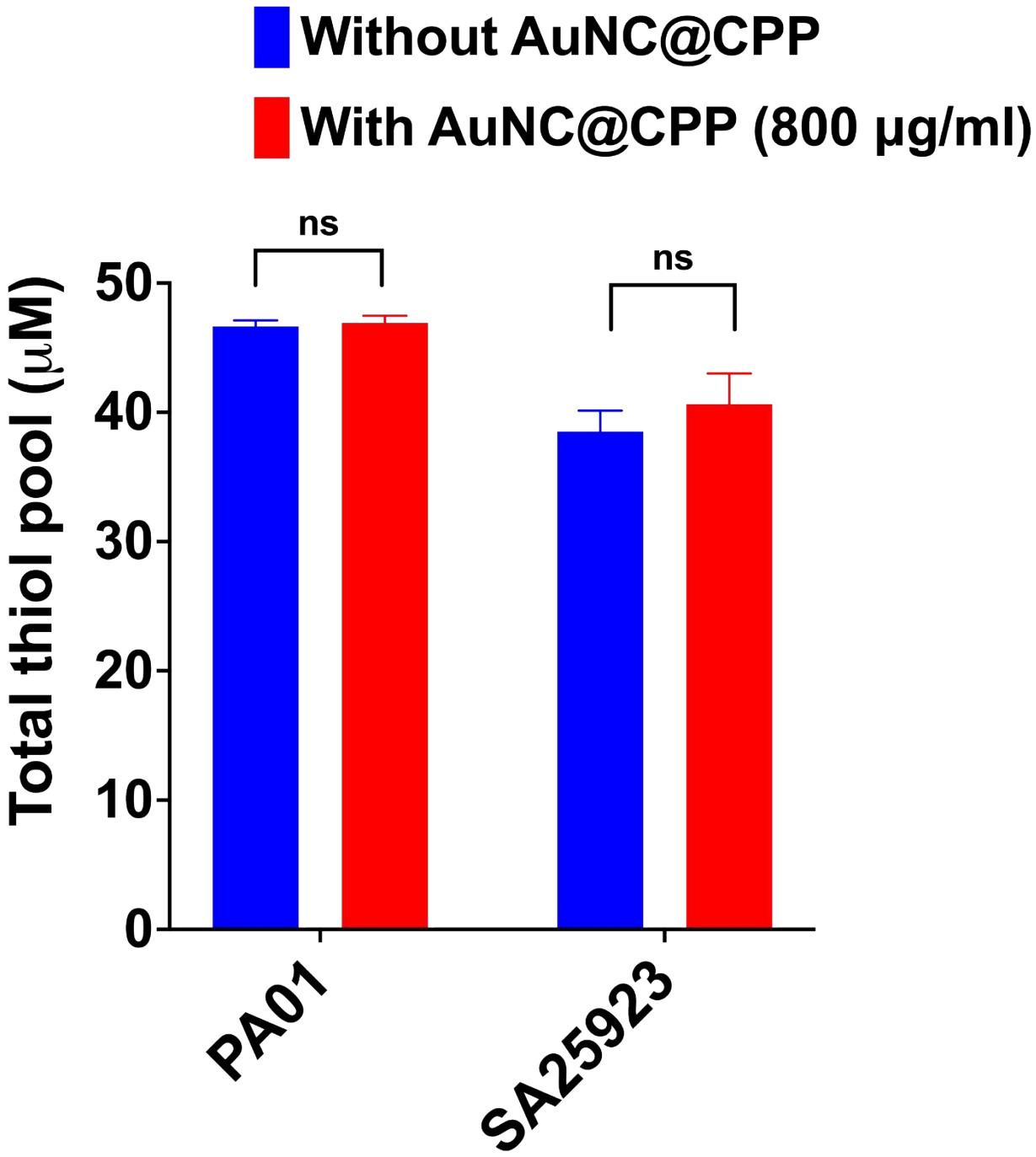

Fig. S5 AuNC@CPP does not cause thiol depletion in bacteria. The corresponding thiol levels following the treatment of PA01 and SA25923 with AuNC@CPP (800 µg/mL) for 2 h.

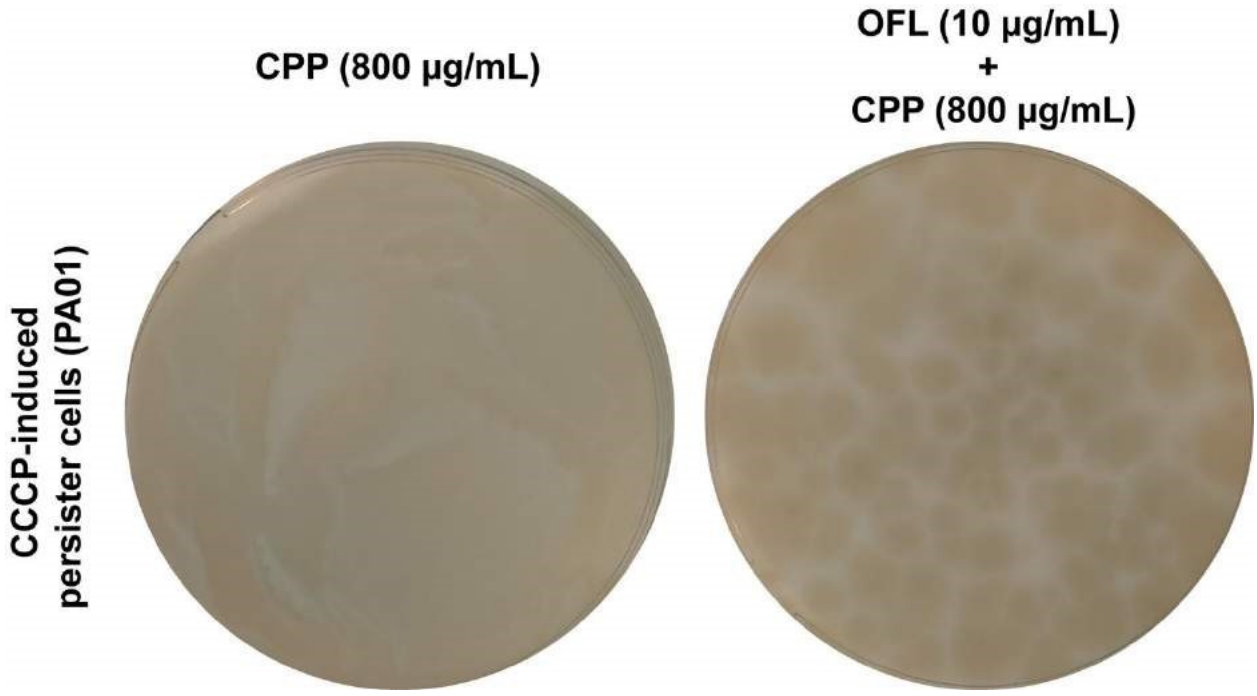

Fig. S6 CPP does not directly contribute to the synergistic effect between AuNC@CPP and antibiotics. Photographs of the agar plate showing the regrowth of CCCP-induced persister cells following with the treatment with CPP (800 µg/mL) and OFL (10 µg/mL) combined with CPP (800 µg/mL) after 24 h treatment. Regrowth was observed in both conditions suggesting that CPP does not play any role in the synergistic effect. The photographs represent Petri dishes from three independent experiments (n= 3) for each condition.

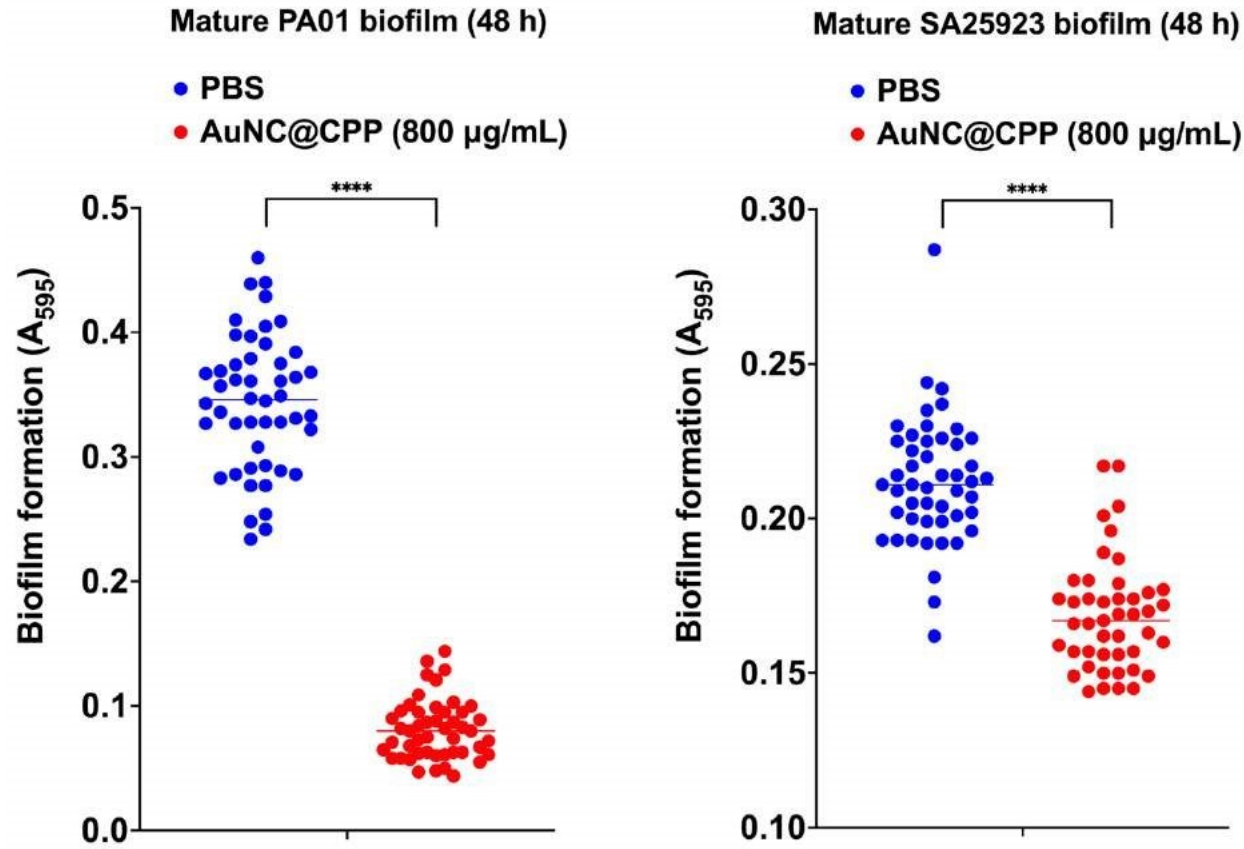

Fig. S7 AuNC@CPP dissociates the preformed biofilm. 48 h old biofilm of PA01 and SA25923 was treated with AuNC@CPP (800 µg/mL) for 24 h. The biofilm biomass was quantified using the crystal violet staining, and a significant decrease in the biofilm was observed between the PBS and AuNC@CPP treatment groups, suggesting that AuNC@CPP dislocates the biofilm.

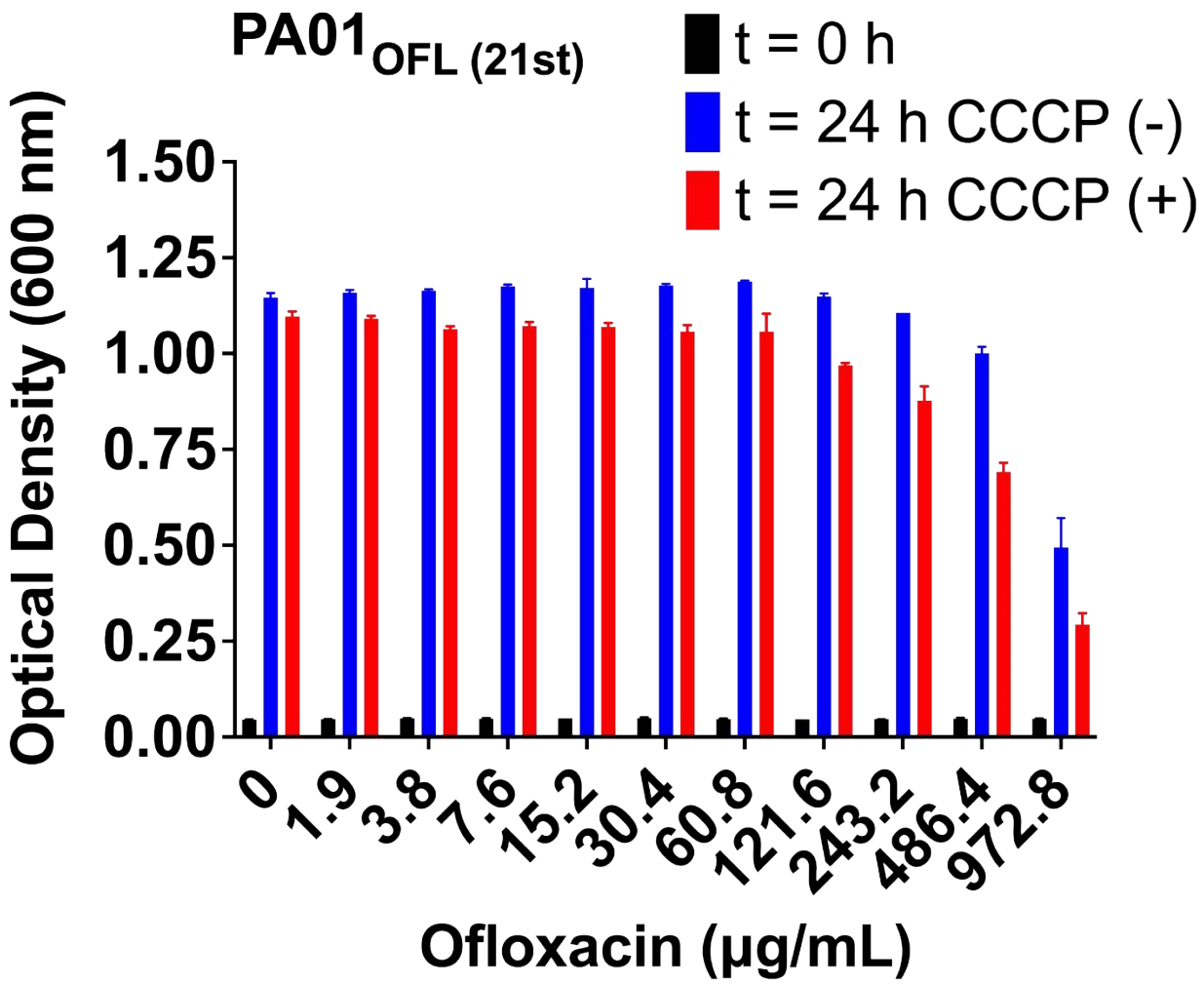

Fig. S8 Efflux pumps do not contribute to the resistance mechanism. MIC of the PA01 passage 21st was determined in the absence and presence of efflux pump inhibitor (CCCP = 20 µg/mL). There is no decrease in MIC in the presence of CCCP.

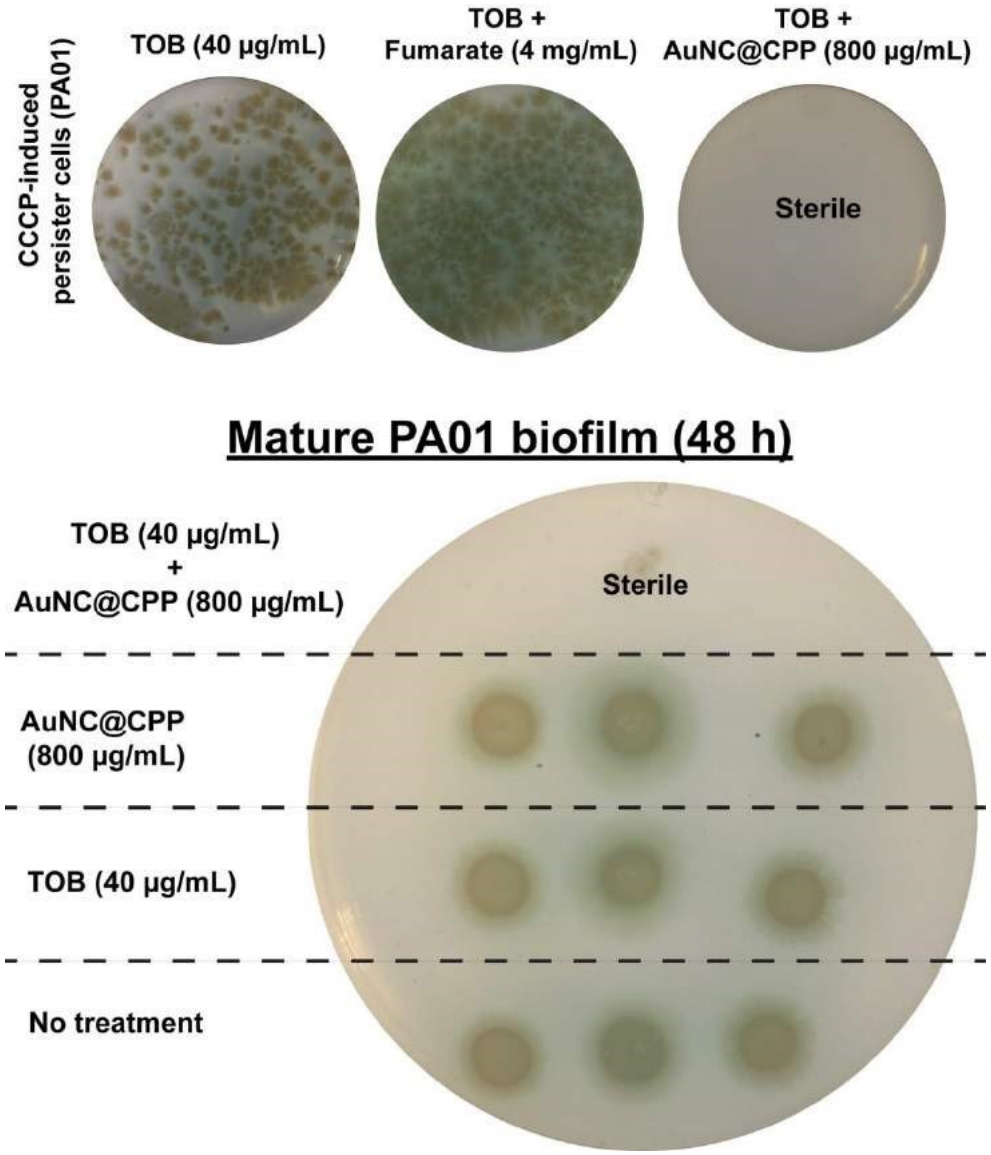

Fig. S9 AuC@CPP enables the eradication of persister cells and mature biofilms by tobramycin (TOB). Representative petri dish showing regrowth of persister cells following treatment of CCCP-induced persister cells with TOB (40 µg/mL) and TOB (40 µg/mL) combined with either fumarate (4000 µg/mL) or AuNC@CPP (800 µg/mL). Following the treatment, the entire bacterial pellet was suspended in 100 µL of PBS, plated in agar, and incubated for up to 72 h to confirm the sterilization. No viable persister cells were found if TOB were combined with AuNC@CPP. The images represent Petri dishes from three independent experiments (n= 3) for each condition. (bottom) Representative petri dish showing persister cells resuscitation following treatment of 48h-old PA01 biofilms by TOB (40 µg/mL), AuNC@CPP (800 µg/mL), and their combination for 24 h. The recovery media (10 µL) was inoculated on the Petri dishes and incubated at 37 ºC for 72 h. The images represent Petri dishes from three independent experiments (n= 3) for each condition. If TOB is combined with AuNC@CPP, no viable biofilm cells were found.

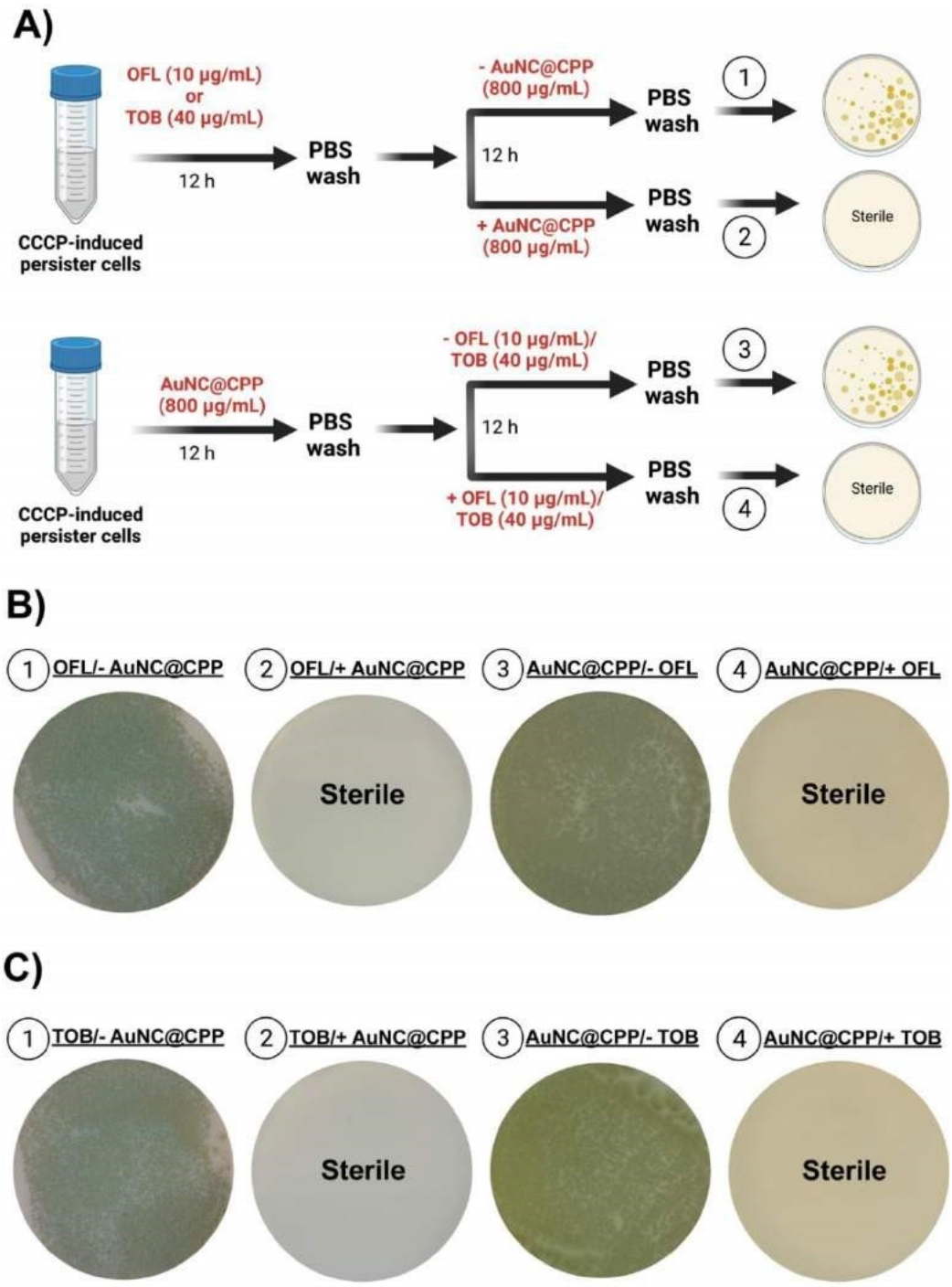

Fig. S10 Synergistic effect between antibiotics and AuNC@CPP occurs regardless of treatment order. (A) Schematic illustration of the sequential treatment of CCCP-induced persister cells with either OFL or TOB and AuNC@CPP in interchangeable order. (B) No viable CCCPinduced persister cells were found following the sequential treatment in interchangeable order with OFL (10 µg/mL) and AuNC@CPP (800 µg/mL). (C) No viable CCCP-induced persister cells
were found following the sequential treatment in interchangeable order with TOB (40 µg/mL) and

AuNC@CPP (800 µg/mL).

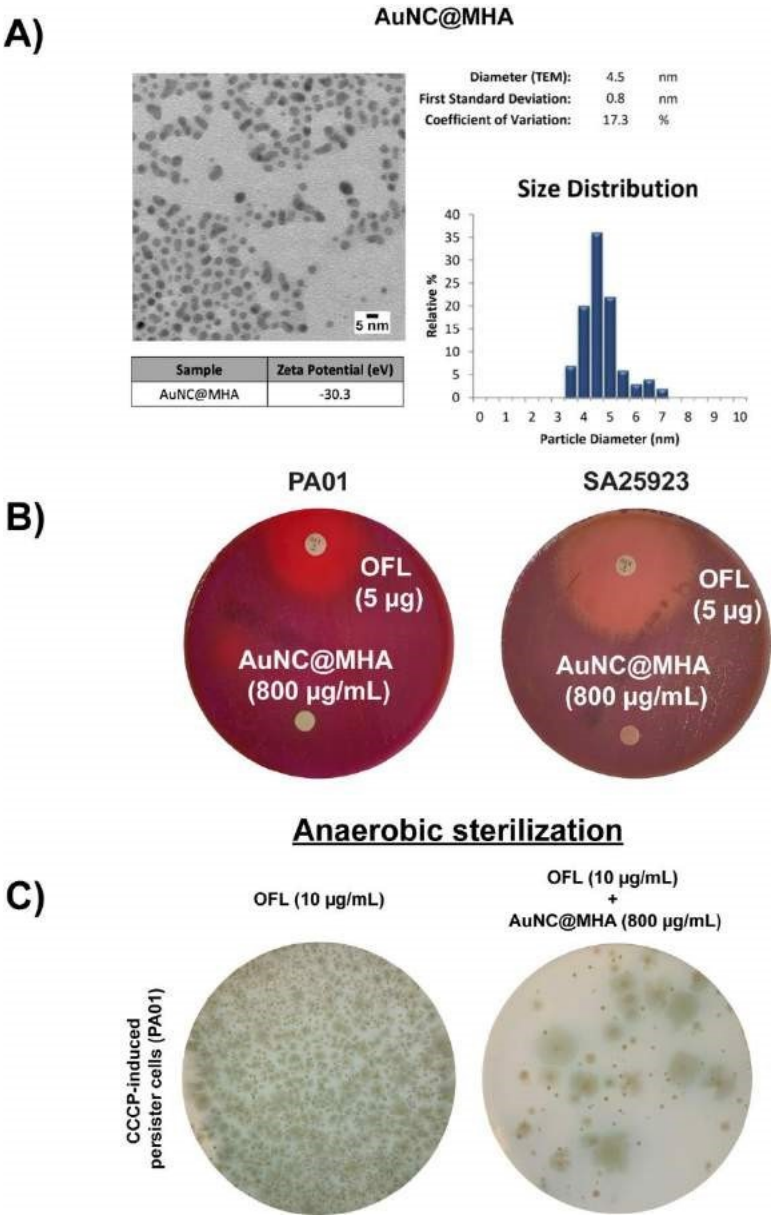

Fig. S11 Surface chemistry is not crucial to the synergy between antibiotic and gold nanoclusters. **(A)** TEM image of AuNC@MHA and the size distribution with a coefficient of variation equal to 25.1%. The zeta potential of AuNC@MHA was measured in water at pH 7. (B) Photographs of the disk diffusion test show the zone of inhibition around OFL, but AuNC@MHA has no antimicrobial activity against Gram-negative (PA01) and Gram-positive (SA25923). (C) Representative petri dish showing regrowth of persister cells following treatment of CCCPinduced persister cells with OFL (10 µg/mL) in the absence and presence of AuNC@MHA (800 µg/mL). Following the treatment, the entire bacterial pellet was suspended in 100 µL of PBS, plated in agar, and incubated for up to 72 h to confirm the sterilization. If OFL is combined with AuNC@CPP (800 µg/mL), A negligible amount of viable CCCP-induced persister cells were found compared to OFL. The images represent Petri dishes from three independent experiments (n= 3) for each condition.

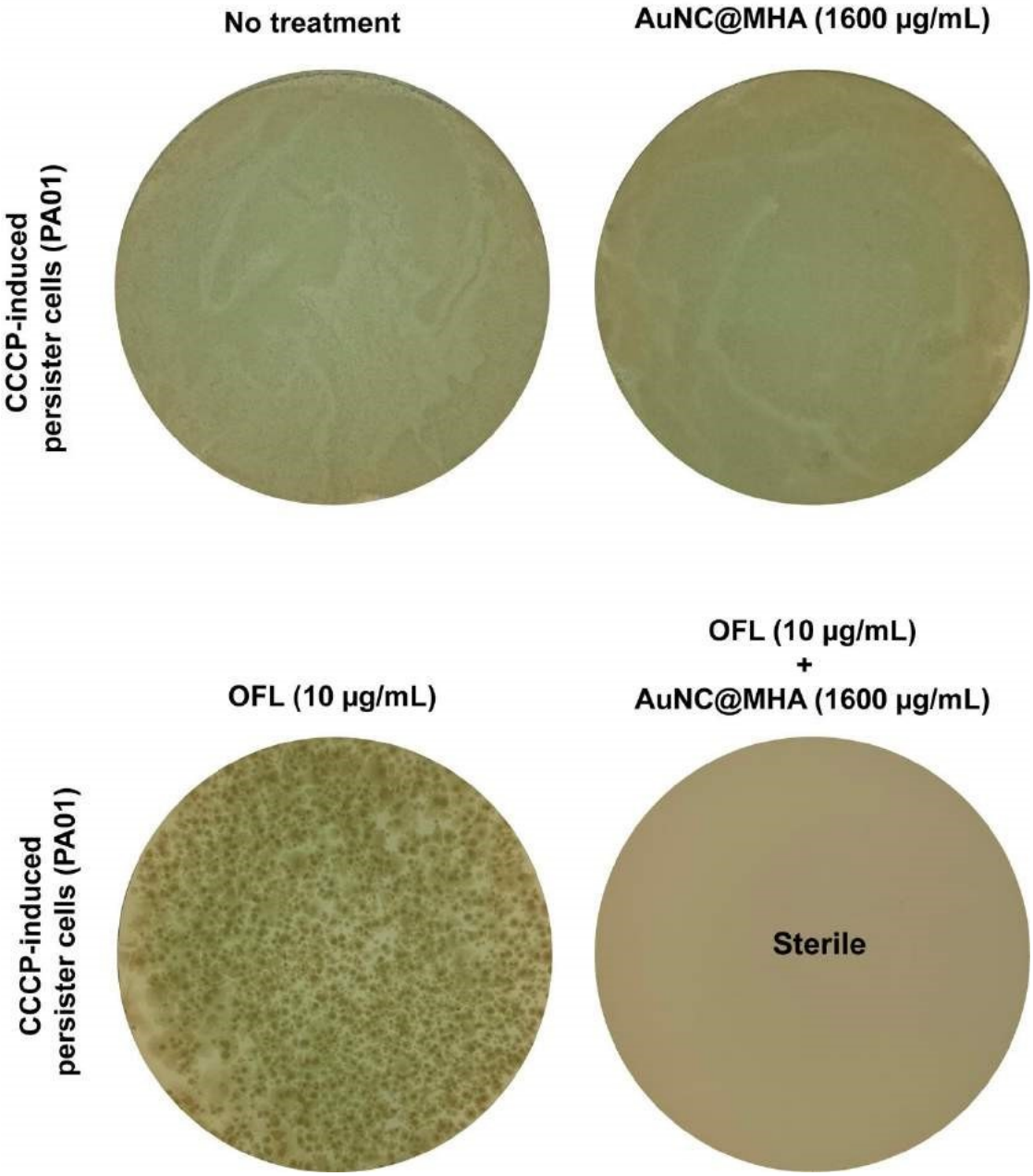

Fig. S12 High concentration of AuNC@MHA potentiates persister cell eradication by OFL. Representative petri dish showing regrowth of persister cells following treatment of CCCPinduced persister cells with OFL (10 µg/mL) in the absence and presence of AuNC@MHA (1600 µg/mL). Following the treatment, the entire bacterial pellet was suspended in 100 µL of PBS, plated in agar, and incubated for up to 72 h to confirm the sterilization. If OFL is combined with AuNC@MHA (1600 µg/mL), A negligible amount of viable CCCP-induced persister cells were found compared to OFL. The images represent Petri dishes from three independent experiments (n= 3) for each condition.

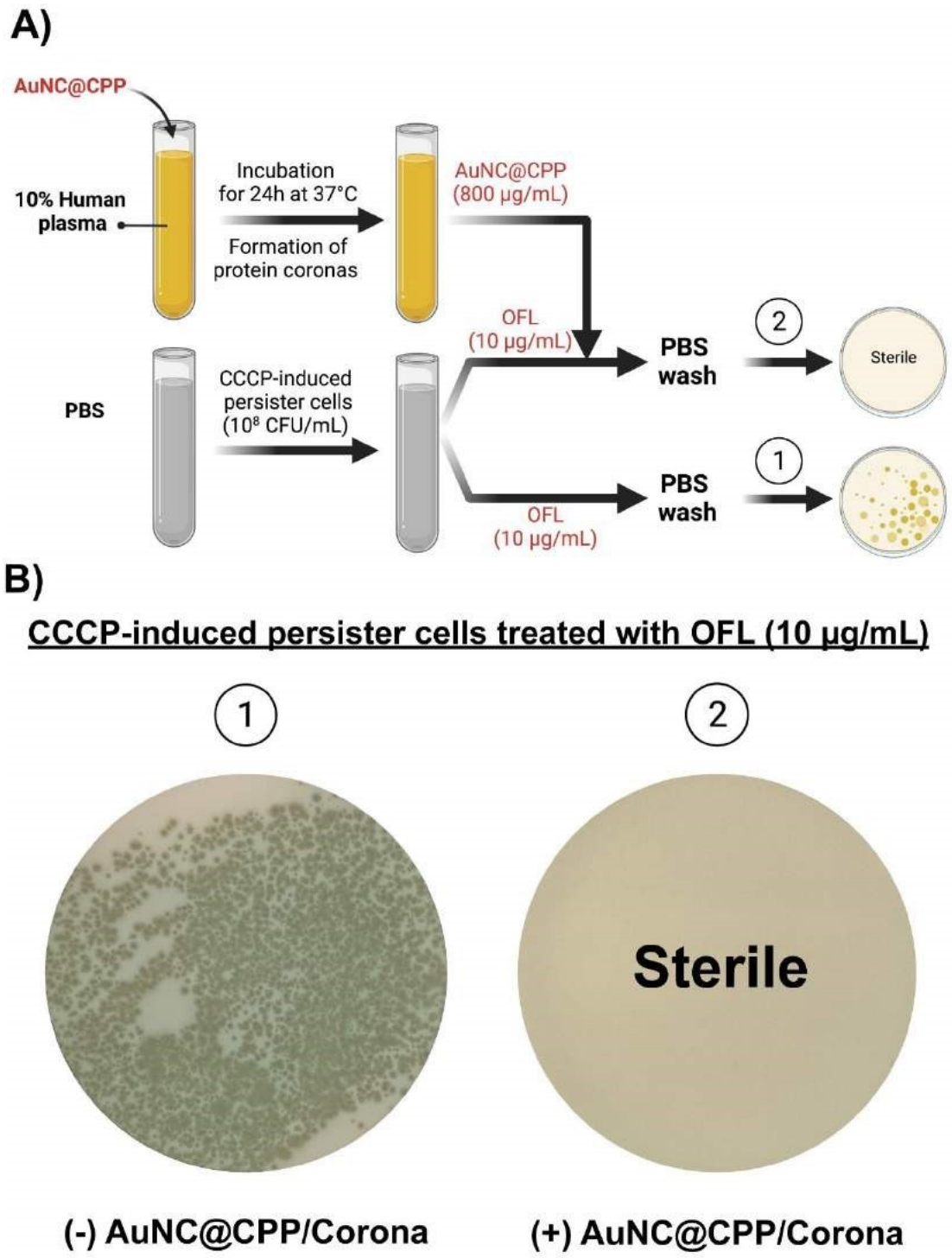

Fig. S13 The protein corona does not abolish the synergistic effect between antibiotics and AuNC@CPP. (A) Schematic illustration of the preparation of protein corona and eradication of CCCP-induced persister cells with OFL in the absence and presence of AuNC@CPP/corona. (B) If OFL is combined with AuNC@CPP (800 μg/mL), no viable CCCP-induced persister cells were found.

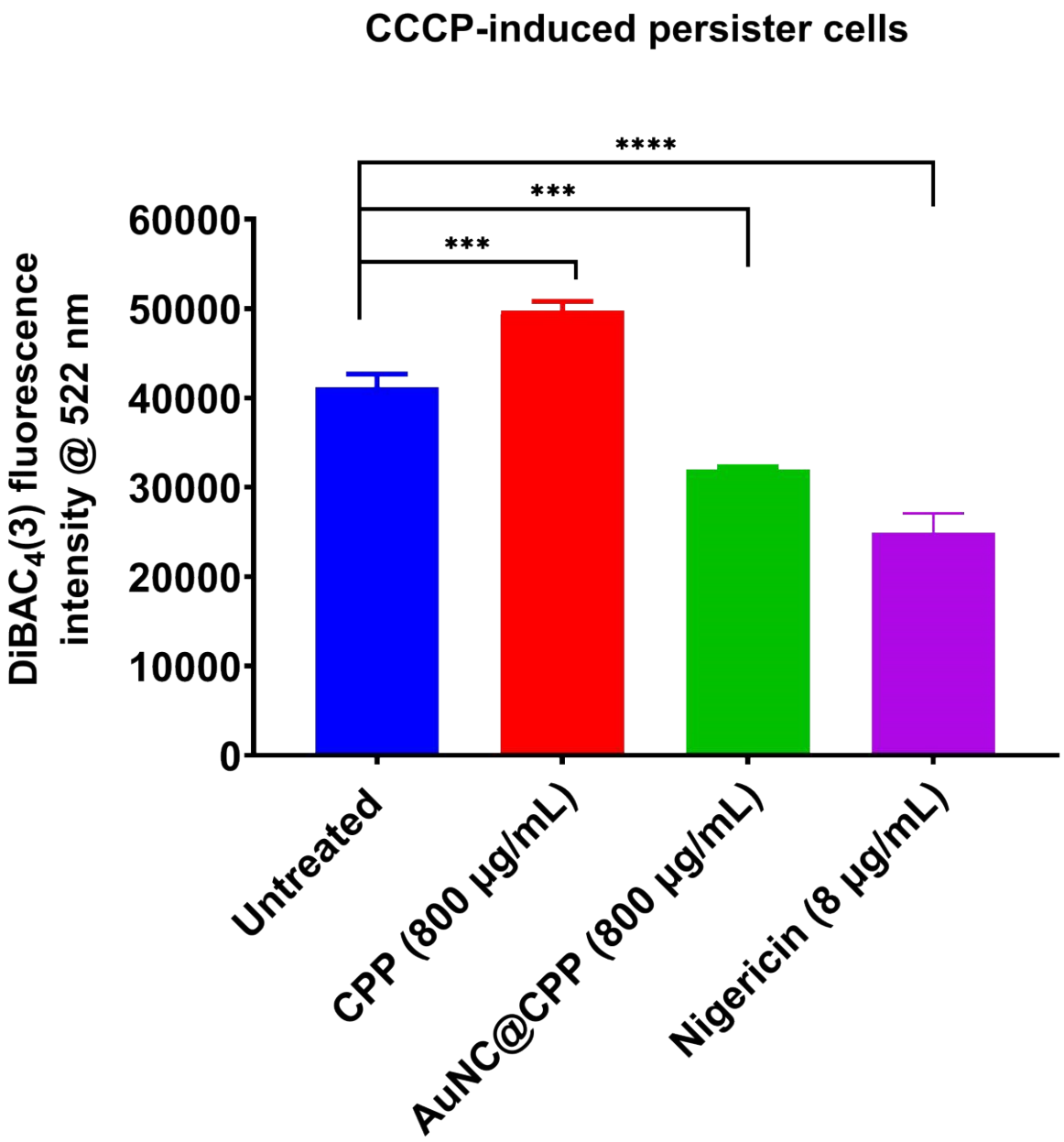

Fig. S14 The AuNC@CPP-induced hyperpolarization of the membrane. The hyperpolarizing effect is demonstrated by the decrease in the $DiBAC_4$ (3) fluorescence intensity value compared to the untreated control.

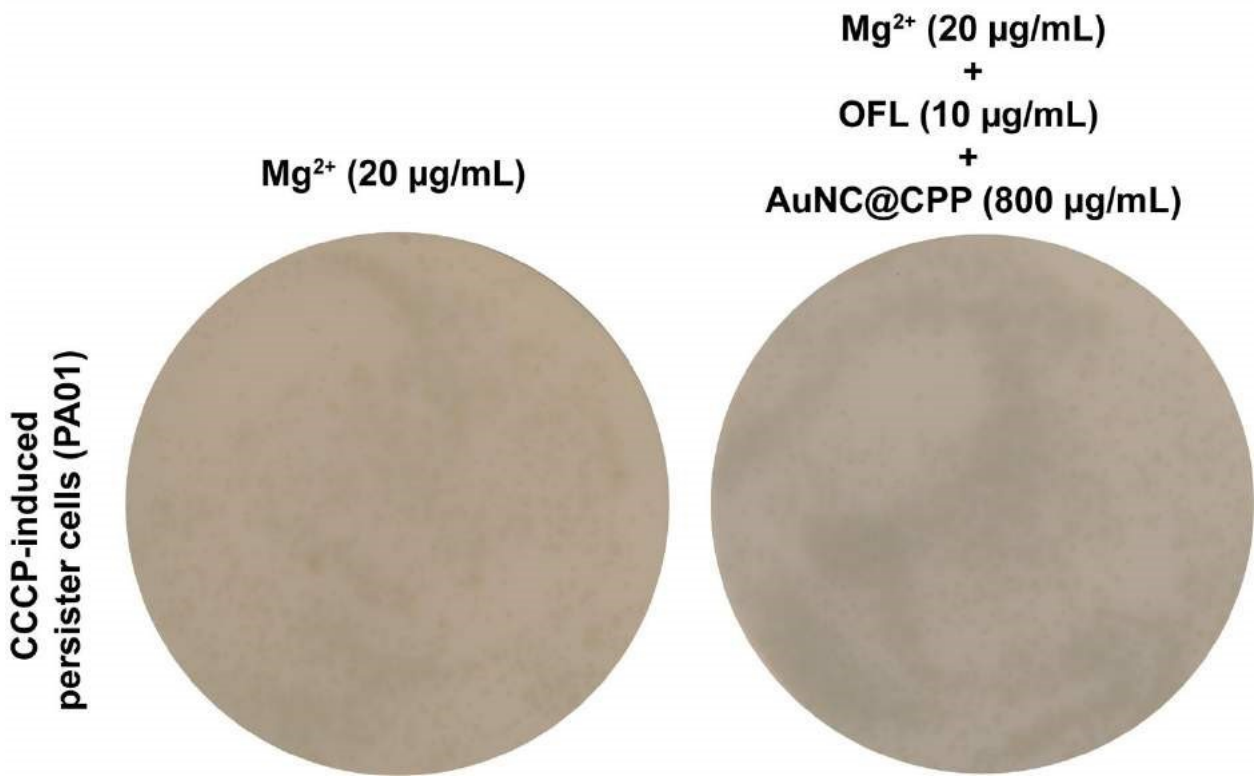

Fig. S15 Disruption of membrane hyperpolarization by adding magnesium (Mg^{2+}) eliminates the synergistic effect between AuNC@CPP and antibiotics. Mg^{2+} removes the membrane hyperpolarization induced by AuNC@CPP. Photographs of the agar plate showing the regrowth of CCCP-induced persister cells following with the treatment with Mg^{2+} (20 µg/mL) and Mg^{2+} (20 µg/mL) combined with OFL (10 µg/mL) and AuNC@CPP (800 µg/mL) after 24 h treatment. Regrowth was observed in both conditions suggesting that membrane hyperpolarization is the leading cause of the synergistic effect. The photographs represent Petri dishes from three independent experiments (n= 3) for each condition.